J|A|C|S COMMUNICATIONS

Published on Web 09/14/2010

A New in Situ Optical Microscope with Single Atomic Layer Resolution for Observation of Electrochemical Dissolution of Au(111)

Rui Wen,[†] Abhishek Lahiri,[†] Mukkannan Azhagurajan,[†] Shin-ichiro Kobayashi,[‡] and Kingo Itaya*[,†,‡]

World Premier International Research Center, Advanced Institute for Materials Research (WPI-AIMR), Tohoku University, Katahira 2-1-1, Aobaku, Sendai 980-8577, Japan, and Department of Applied Chemistry, Graduate School of Engineering, Tohoku University, 6-6-04 Aoba, Sendai 980-8579, Japan

Received July 14, 2010; E-mail: itaya@atom.che.tohoku.ac.jp

Abstract: Monatomic steps with a height of 0.25 nm on ultraflat Au(111) surfaces during electrochemical dissolution can be seen for the first time by a laser confocal microscope combined with a differential interference contrast microscope (LCM-DIM). Atomic force microscopy images were acquired in the same area in order to confirm that the step lines observed by LCM-DIM are mostly monatomic steps with the height of 0.25 nm. Successively recorded LCM-DIM images indicated that the anodic dissolution of Au(111) takes place only at step edges in solutions containing chloride anions at potentials near the onset of anodic current.

Scanning probe microscopic techniques such as scanning tunneling microscopy (STM) and atomic force microscopy (AFM) make it possible to monitor, under reaction conditions, a wide variety of electrode processes such as the adsorption of inorganic and organic species, the reconstruction of electrode surfaces, and the dissolution and deposition of metals and semiconductors.[1−4] However, there are several limitations in these scanning probe techniques. For example, probes such as the tunneling tip in STM and the cantilever in AFM measurements may interfere with electrochemical processes. Several papers pointed out that the scanning movement of the tip in STM might disturb the concentration distribution of the solute in the vicinity of the electrode surface, affecting the crystal growth kinetics.[5,6] Similar unfavorable effects have also been found in the evaluation of crystal growth of organic materials in solution.[7] The other limitation in STM and AFM is the relatively small observable scan areas, typically only a few tenths of a micrometer square. This limitation makes it difficult to understand the overall aspect of electrochemical reactions taking place in the entire area of a real electrode surface. Furthermore, typical long acquisition times more than several minutes also make it difficult to follow relatively fast reactions taking place on electrode surfaces, although video-rate in situ STM has been recently developed by Magnussen's group.[8,9]

It has long been desired to develop an optical microscopy technique that gives atomic-scale information for the evaluation of electrochemical reactions in order to overcome these problems. Among several new types of optical microscopes employed to observe elemental steps on solid surfaces and the subsurface structure of living cells,[10−14] a laser confocal microscope combined with a differential interference contrast microscope (LCM-DIM) has been recently demonstrated to be capable of resolving monomolecular steps on single crystals of biological materials, even in solution.[7,15,16] Although Sazaki's group reported for the first time that the elementary growth steps (5.6 nm in height) on the {110} surfaces of a tetragonal lysozyme crystal in aqueous solutions can be seen relatively easily by LCM-DIM,[15] the resolution in the *z*-direction must be increased by an order of magnitude for the purpose of observing monatomic steps on Au(111) surfaces, because the height of monatomic steps of metals commonly of interest is usually less than 0.3 nm. In our recent paper, we showed that monatomic steps on Pd(111) (0.23 nm in height) and Au(111) (0.25 nm in height) can be clearly seen by our LCM-DIM in air and even in solutions.[17]

In the present paper, we reveal that the anodic dissolution process of Au(111) in solutions containing chloride anions can be directly observed over a large area (more than $100 \times 100\ \mu m^2$) by LCM-DIM. It is clearly shown that the anodic dissolution takes place only at step edges at potentials near the onset of anodic current.

Our system is constructed by attaching a confocal system (FV300, Olympus) to an inverted optical microscope (IX70, Olympus), equipped with a Nomarski prism introduced into the optical path and a partially coherent superluminescent diode (Amonics Ltd., model ASLD68-050-B-FA: 680 nm) to eliminate interference fringes, which is basically the same as that reported by Sazaki's group,[7,18] although several improvements have been made in the present study. Note that the acquisition time of each image of LCM-DIM is typically a few seconds. A more detailed experimental setup is included in the Supporting Information. AFM images of Au(111) surfaces were obtained by using a PicoSPM 5500 (Agilent Corp.).

During sample preparation, it is necessary to prepare a very flat Au(111) surface, having terrace widths greater than several micrometers, because the lateral resolution of the LCM-DIM method is limited to the range of 0.2−0.3 μm by the wavelength of the monitoring light, as in conventional optical microscopy.[17] Spherical single-crystal beads of gold were obtained by melting the end of a Au wire (99.999% purity, 0.8 mm diameter) in a H_2/O_2 flame as described previously.[19,20] A photograph of the single-crystal bead in full scale is included as Figure 1 in the Supporting Information.

In the present study, the Au single-crystal beads were further annealed in an electromagnetic furnace (HOTSHOT5, Ambrell Ltd.) in a temperature range of 600−800 °C under purified argon atmosphere to obtain the ultraflat surface. This annealing method is superior to that used to obtain evaporated Au films on mica frequently used for STM studies,[21,22] because the terrace widths on these films were normally smaller than the terrace widths observed on the Au(111) facet.

Figure 1A shows a typical AFM image acquired on an area of $1 \times 1\ \mu m^2$, on a normal Au(111) facet on the single-crystal bead, which was prepared by the conventional H_2/O_2 flame procedure.[19] The surface was composed of an atomically flat terrace-step

[†] WPI-AIMR.
[‡] Department of Applied Chemistry.

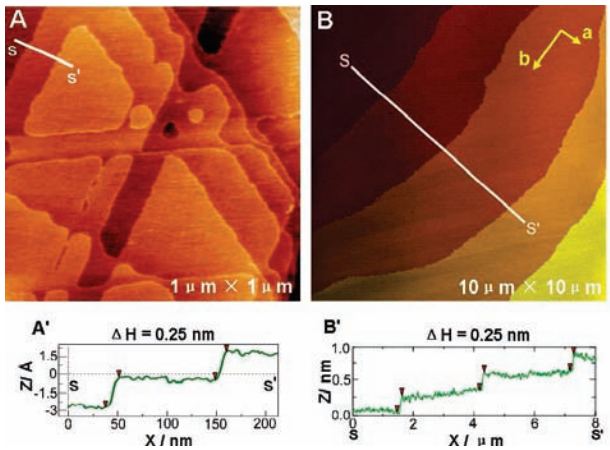

Figure 1. AFM images on normal Au(111) (A) and ultraflat Au(111) (B) surfaces. Line profiles shown in (A′) and (B′) indicate cross sections along the lines shown in (A) and (B), respectively. The images were obtained in 4.3 (A) and 12 min (B).

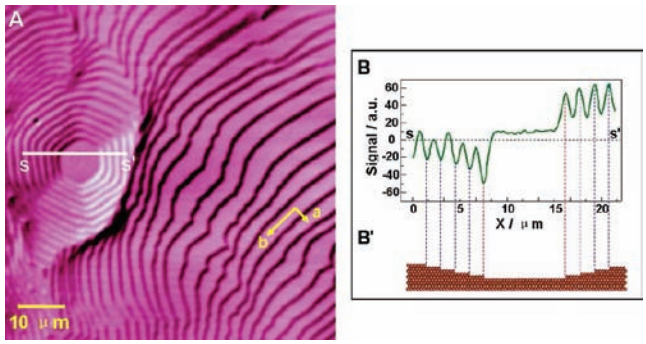

Figure 2. LCM-DIM image (A) of a typical ultraflat Au(111) surface in air with a scan area of 70 × 70 μm^2. The cross-section profile (B) reveals the signal intensity along the line in (A). A side model of the surface structure along the line is presented in (B′). The image was obtained in 2.4 s.

structure with monatomic steps with a height of 0.25 nm, as shown by the line profile along the line in Figure 1A, while the widths of atomically flat terraces were in the range of 50−500 nm. However, the atomically flat terraces were not wide enough for observation by the LCM-DIM method, because of the limitation of the lateral resolution of the LCM-DIM method.

On the other hand, Figure 1B shows a typical AFM image for annealed ultraflat Au(111) facets acquired on a scan area of 10 × 10 μm^2. It can be seen that the terrace widths of the annealed Au(111) facets are surprising larger than those of the normal Au(111) facets before annealing as shown in Figure 1A. Terrace widths in the directions indicated by arrows **a** and **b** are 2−5 and >10 μm, respectively, as shown in Figure 1B. Note that the well-defined steps were found to be all monatomic, as shown by a line profile in Figure 1B.

After characterization of the surface morphology by AFM, we subjected the same ultraflat Au(111) surface to an examination by LCM-DIM. A typical image obtained by LCM-DIM is shown in Figure 2A, in which the observed area was as large as 70 × 70 μm^2. The acquisition time was very short (2.4 s) compared with those of the AFM images shown in Figure 1. It is remarkable that regularly aligned step lines are clearly discerned. According to the result shown in Figure 1B, these step lines must be monatomic steps on Au(111). The output of signal intensity of LCM-DIM along the direction of the S−S′ line in Figure 2A is shown in Figure 2B. The downward and upward atomic steps appear as dark and bright

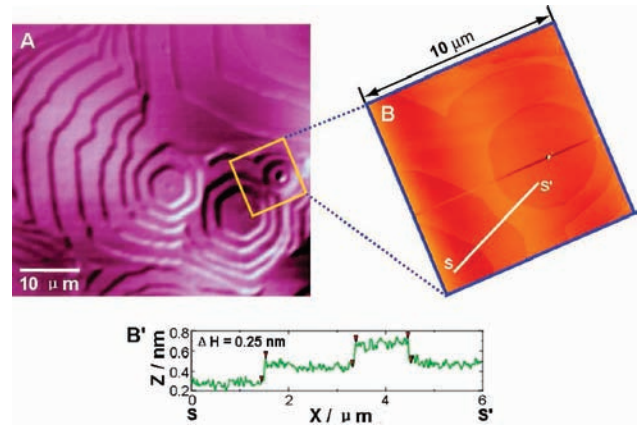

Figure 3. Comparison of LCM-DIM image (A) on ultraflat Au(111) and AFM image (B) of the area marked by the square of 10 × 10 μm^2 in (A). A line profile along the line S−S′ is shown in (B′). LCM-DIM and AFM images were obtained in 2.4 s and 8.5 min, respectively.

lines, respectively. The signal intensity in LCM-DIM decreases at the downward steps, as seen in the cross-section profile in Figure 2B. A side model surface structure along the S−S′ line of Au(111) is illustrated in Figure 2B′. The terrace width along the direction **a** is about 2−5 μm, consistent with the AFM result shown in Figure 1B, whereas the width in direction **b** extends more than 70 μm.

To confirm that the step lines observed by LCM-DIM are mostly monatomic steps, AFM images of the same area were acquired and compared each other. Figure 3A shows an LCM-DIM image acquired with an ultraflat sample prepared for a longer annealing time. It is seen that terraces observed by LCM-DIM were as wide as several tens of micrometers, suggesting that annealing conditions are crucial in the preparation of ultraflat Au(111). An AFM image of the area defined by the square mark of 10 × 10 μm^2 in LCM-DIM image of Figure 3A was obtained within 1 h, as shown in Figure 3B. In this defined area, the shape of step lines is almost identical in both LCM-DIM and AFM images. Note that all step lines in the AFM image shown in Figure 3B are monatomic in height. A line profile along the S−S′ line in Figure 3B is shown in Figure 3B′. These results confirm that the step lines observed by LCM-DIM shown in Figure 3A are mostly monatomic steps; thus, it is concluded that LCM-DIM can resolve monatomic steps on a Au(111) surface. Furthermore, it is shown that a composite AFM image constructed from nine AFM images has the same shape of step lines observed by LCM-DIM (see Figure 3 in the Supporting Information).

It is well-recognized that the evaluation of electrochemical reactions such as dissolution and deposition of metals is an important subject in electrochemistry from both fundamental and practical viewpoints.[23−25] For example, anodic dissolution processes of Cu,[26] Au,[19,27] and Pd[28] have been investigated using in situ STM, revealing the electrode processes at atomic level under the reaction conditions.

The results described above prompted us to investigate electrochemical reactions taking place on solid surfaces with atomic step resolution by using the LCM-DIM method. In this study, the anodic dissolution of Au was investigated in an acid solution containing chloride ions. Figure 4A shows cyclic voltammograms (CVs) of a Au(111) electrode in 0.1 M $HClO_4$ in the absence (black line) and in the presence of 3 mM HCl (red line). In 0.1 M $HClO_4$ containing no chloride ions, the two main oxidation peaks observed at 1.35 and 1.55 V vs RHE correspond to the oxidation of the first layer of Au(111), according to the following reactions.[19,29]

$$Au + H_2O \rightarrow Au^{I}OH + H^+ + e^- \quad (1)$$

$$Au^{I}OH \rightarrow Au^{II}O + H^+ + e^- \quad (2)$$

The cathodic peak at ca. 1.15 V is due to the reduction of the Au oxide ($Au^{II}O$). The anodic dissolution of Au does not occur in 0.1 M $HClO_4$ in the potential range of Figure 4A. These results are consistent with those of previous studies.[19,29] On the other hand, in the presence of chloride anions, the anodic current arising at ca. 1.3 V is due to the anodic dissolution of Au, according to the following reaction:[19,27,30]

$$Au + 4Cl^- \rightarrow [Au^{III}Cl_4]^- + 3e^- \quad (3)$$

A characteristic terrace-step structure in 3 mM HCl and 0.1 M $HClO_4$ can be seen by LCM-DIM at potentials less than 1.2 V, as shown in Figure 4B. Almost identical images were consistently observed when the electrode potential was kept at a value more negative than 1.2 V. However, when the electrode potential was set at a value close to the onset of the anodic dissolution, it was found that all step lines were retracted toward the inner part of each terrace, suggesting that the anodic dissolution took place at step edges. Figure 4C,D shows time-dependent LCM-DIM images of the anodic dissolution process of the Au(111) surface. In addition to the series of monatomic steps, several pits with a monatomic depth can also be seen on terraces, which are marked by yellow arrows in Figure 4B. The three pits seen in the corresponding enlarged image in Figure 4B′ increased in size gradually due to the dissolution, and finally these pits combined together to form a new large pit, as shown in Figure 4C′,D′. Steps mostly monatomic in height characterized by an arc shape (rather than straight) retracted by ca. 150 nm/min as an averaged rate. On the other hand, straight steps retracted by ca. 100 nm/min (see Figure 4 in the Supporting Information). The density of kinks may play a role in controlling the etching rate. Finally, note that no new pits were formed under the present experimental conditions, as shown in Figure 4, while new pits were found to form at more positive potentials. The etching rate of step lines was also increased. A more detailed study is now under investigation.

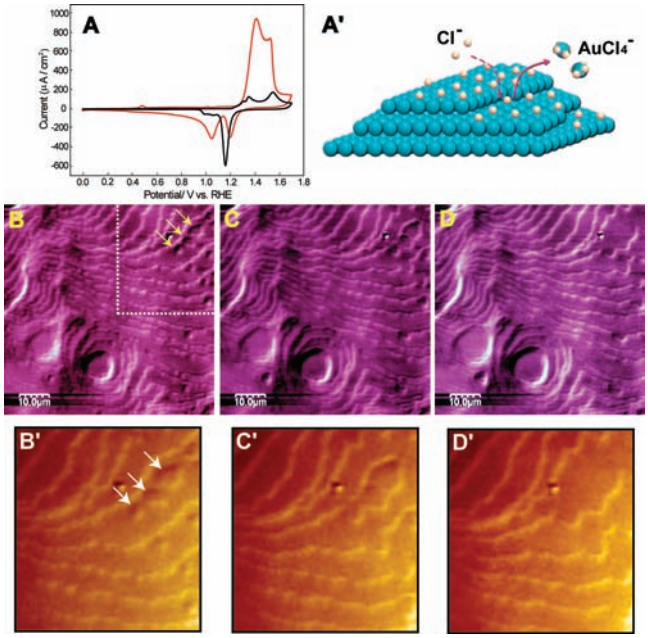

Figure 4. Cyclic voltammograms of Au(111) electrode in 0.1 M $HClO_4$ in the absence (black line) and in the presence of 3 mM HCl (red line) (A), scan rate 50 mV/s. In situ LCM-DIM observation of the process of anodic dissolution of Au(111) was carried out in 3 mM HCl + 0.1 M $HClO_4$ at 1.2 V (B) and then 10 min later (C) and 15 min later (D) at 1.3 V. Each image was obtained in 2.4 s. (B′), (C′), and (D′) are the corresponding enlarged areas of the top right corners marked by the squares in (B), (C), and (D). The anodic dissolution at step edges is illustrated in (A′). (See video in the Supporting Information to view the dynamic process.)

We conclude that LCM-DIM is a new powerful in situ method for evaluating various electrochemical reactions with single atomic layer resolution.

Acknowledgment. The authors acknowledge Prof. G. Sazaki (Hokkaido Univ.) and Mr. Y. Saito (Olympus) for developing the LCM-DIM system. This work was supported by the Ministry of Education, Culture, Sports, Science and Technology of Japan under Grant No. 20245038 and in part by the New Energy and Industrial Technology Development Organization (NEDO).

Supporting Information Available: Additional figures and movie showing gold dissolution. This material is available free of charge via the Internet at http://pubs.acs.org.

References

(1) Gewirth, A. A.; Niece, B. K. *Chem. Rev.* **1997**, *97*, 1129–1162.
(2) Itaya, K. *Prog. Surf. Sci.* **1998**, *58*, 121–248.
(3) Siegenthaler, H. In *Scanning Tunneling Microscopy II*; Wiesendanger, R., Guntherodt, H. J., Eds.; Springer-Verlag: Berlin, 1992.
(4) Wang, D.; Wan, L. J. *J. Phys. Chem. C* **2007**, *111*, 16109–16130.
(5) Andersen, J. E. T.; Bech-Nielsen, G.; Møller, P.; Reeve, J. C. *J. Appl. Electrochem.* **1996**, *26*, 161–170.
(6) Nichols, R. J.; Kolb, D. M.; Behm, R. J. *J. Electroanal. Chem.* **1991**, *313*, 109–119.
(7) Driessche, A. E. S. V.; Otalora, F.; Sazaki, G.; Sleutel, M.; Tsukamoto, K.; Gavira, J. A. *Cryst. Growth Des.* **2008**, *8*, 4316–4323.
(8) Taranovskyy, A.; Tansel, T.; Magnussen, O. M. *Phys. Rev. Lett.* **2010**, *104*, 106101–106104.
(9) Tansel, T.; Magnussen, O. M. *Phys. Rev. Lett.* **2006**, *96*, 026101−026104.
(10) Nishizawa, J.; Tadano, H.; Oyama, Y.; Shimbo, M. *J. Cryst. Growth.* **1981**, *55*, 402–405.
(11) Hottenhuis, M. H. J.; Van den Berg, A. L. M.; Van der Eerden, J. P. *Electrochim. Acta* **1988**, *33*, 1519–1538.
(12) Tsukamoto, K.; Dold, P. In *Perspectives on Inorganic, Organic, and Biological Crystal Growth: From Fundamentals to Applications*; Skowronski, A., DeYoreo, J. J., Wang, C., Eds.; American Institute of Physics: Melville, NY, 2007; pp 329−341.
(13) Popescu, G. In *Quantitative Phase Imaging of Nanoscale Cell Structure and Dynamics*; Jena, B. P., Ed.; Methods in Nano Cell Biology *90*; Elsevier: Burlington, VT, 2008.
(14) Depeursinge, C. In *Digital Holography and Three-Dimensional Display-Principles and Applications*; Poon, T.-C., Ed.; Springer: New York, 2006.
(15) Sazaki, G.; Matsui, T.; Tsukamoto, K.; Usami, N.; Ujihara, T.; Fujiwara, K.; Nakajima, K. *J. Cryst. Growth.* **2004**, *262*, 536–542.
(16) Driessche, A. E. S. V.; Sazaki, G.; Otalora, F.; Gonzalez-Rico, F. M.; Dold, P.; Tsukamoto, K.; Nakajima, K. *Cryst. Growth Des.* **2007**, *7*, 1980–1987.
(17) Wen, R.; Lahiri, A.; Azhagurajan, M.; Kuzume, A.; Kobayashi, S.; Itaya, K. *J. Electroanal. Chem.*, in press.
(18) Suzuki, Y.; Sazaki, G.; Matsumoto, M.; Nagasawa, M.; Nakajima, K.; Tamura, K. *Gryst. Growth. Des.* **2009**, *9*, 4289–4295.
(19) Honbo, H.; Sugawara, S.; Itaya, K. *Anal. Chem.* **1990**, *62*, 2424–2429.
(20) Clavilier, J.; Faure, R.; Guinet, G.; Durand, R. *J. Electroanal. Chem.* **1980**, *107*, 205–209.
(21) Lüssem, B.; Karthäuser, S.; Haselier, H.; Waser, R. *Appl. Surf. Sci.* **2005**, *249*, 197–202.
(22) Nogues, C.; Wanunu, M. *Surf. Sci.* **2004**, *573*, L383–L389.
(23) Herrero, E.; Buller, L. J.; Abruna, H. D. *Chem. Rev.* **2001**, *101*, 1897–1930.
(24) Budevski, E.; Staikov, G.; Lorenz, W. J. *Electrochemical Phase Formation and Growth: An Introduction to the Initial Stages of Metal Deposition*. VCH Publishers: New York, NY, 1996.
(25) Paunovic, M.; Schlesinger, M. *Fundamentals of electrochemical deposition*, 2nd ed.; John Wiley & Sons, Inc.: Hoboken, NJ, 2006.
(26) Suggs, D. W.; Bard, A. J. *J. Am. Chem. Soc.* **1994**, *116*, 10725–10733.
(27) Ye, S.; Ishibashi, C.; Uosaki, K. *Langmuir* **1999**, *15*, 807–812.
(28) Sashikata, K.; Matsui, Y.; Itaya, K.; Soriaga, M. P. *J. Phys. Chem.* **1996**, *100*, 20027–20034.
(29) Angerstein-Kozlowska, H.; Conway, B. E.; Hamelin, A.; Stoicoviciu, L. *Electrochim. Acta* **1986**, *31*, 1051–1061.
(30) Cadle, S. H.; Bruckenstein, S. *J. Electroanal. Chem.* **1973**, *48*, 325–331.

JA106231X